Memoirs of the Faculty of Engineering, Kyushu University, Vol.69, No.4, December 2009

A Comparison of Analysis Methods for Estimating Directional Wave Spectrum from HF Ocean Radar

by

LUKIJANTO[*], Noriaki HASHIMOTO[**], Masaru YAMASHIRO[***]

(Received November 2, 2009)

Abstract

A comparison of two methods, Bayesian Method (BM) and Modified Bayesian Method (MBM), for estimating directional wave spectra from high frequency (HF) ocean radar has been carried out. In terms of validity and applicability, the two recent approaches are compared theoretically and numerically with the equation derived by Barrick (1972). The results show that the performances of the BM and MBM are adequately good. This comparison suggested that the MBM was more efficient than the BM since the MBM is capable of executing high speed computing and reducing the memory usage. Accordingly, the MBM has a good potential for operational application. The accuracy and suitability of both the methods are also compared to reliable field data of SCAWVEX`s project. The results indicate that the estimated directional spectra by using the BM and MBM well agree with the result from buoy. Although the BM is very time consuming to estimate directional spectra from Doppler spectra, this method is more robust in the presence of noise than the MBM.

Keywords: Bayesian Method, Directional wave spectrum, Spectrum, HF radar, Wave observation, Wave data analysis, Current measurement

1. Introduction

The potential of high frequency (HF) oceanic radar has been recognized since Crombie observed and identified the distinctive features of backscattered Doppler spectra[1)]. The first exact derivation of the formulation was mathematically derived by Barrick retaining to the relationship between the Doppler spectra and the directional wave spectra[2)]. Since then, methods for estimating directional wave spectrum from HF oceanic radar have been developed to interpret the backscatter information in terms of these theoretical relationships.

In principle, ocean wave directional spectra can be estimated from the first and second-order Doppler spectral components by inverting the integral equation which relates ocean wave spectrum

[*] Graduate Student, Department of Maritime Engineering
[**] Professor, Department of Urban and Environmental Engineering
[***] Assistant Professor, Department of Urban and Environmental Engineering

to the Doppler spectrum. A number of approaches have been developed to provide theoretical and numerical formulation for estimating the directional wave spectrum from HF radar. Most, however, are yet unable to reflect practical application. They have been developed so far to estimate directional wave spectrum based on the Barrick's linearized integral equation [3-9], with many of advantages and limitations. As adopted by Lipa and Barrick[8], Wyatt[9], and Howell and Walsh[7], those three studies attempted to estimate directional wave spectrum by employing the linear inversion. On the other hand, Hisaki[6] and Hashimoto methods[3-5] adopted the nonlinear form.

Hashimoto and Tokuda[3] described details of mathematical theory of the Bayesian Method for estimating directional wave spectra. The concept was assumed to be an exponential form having piecewise constant functions with respect to the frequency and the directional angle. The principal advantage of the Bayesian Method, as one of the most accurate and reliable methods provided good accuracy and more powerful result for in-situ measurement[10], is that it can be applied without introducing empirical parameters such as those introduced by Hisaki`s method. Unfortunately, this developed method is currently considered time-consuming for iterative calculation[5].

To resolve this problem, a different approach was considered by Lukijanto et al[11] who expanded another inversion scheme, so called Modified Bayesian Method, for estimating directional wave spectra from HF ocean radar. The proposed method was developed by introducing a similar formulation of Maximum Entropy Principle (MEP) presented by Hashimoto and Kobune[12] which was applied successfully to estimate directional function. Therefore, in terms of suitability and accuracy, it is thus possible to make comparisons between the two developed methods, i.e. Bayesian Method[3] and Modified Bayesian Method[11] (hereafter, BM and MBM respectively). Further, the application of both methods for estimating directional wave spectra from HF radar to actual field data will be described also in this work.

The aim of the present study is focused on evaluating comprehensively the existing analysis approaches of the BM and MBM. The fundamental equations for Doppler and directional wave spectra interpretation is presented in section 2; section 3 reviews these two methods presented and examined in the paper. The numerical computation and simulation, and the verification of the presented methods will be given in section 4 and 5 respectively. Finally, the conclusion is described in section 6.

2. Fundamental Equations

The ocean surface waves consist of various component waves with different frequency and propagation direction. The Doppler spectrum, $\sigma(\omega)$, obtained by HF radar represents the energy distribution of the radio wave signal backscattered by the ocean surface waves at the angular frequency ω, and is expressed by the summation of the first-order component, $\sigma^{(1)}(\omega)$, and the second-order component, $\sigma^{(2)}(\omega)$, i.e., $\sigma(\omega) \approx \sigma^{(1)}(\omega) + \sigma^{(2)}(\omega)$. The relationship between the Doppler spectra and directional wave spectra is mathematically expressed by the following equations for deep water conditions [2]:

$$\sigma^{(1)}(\omega) = 2^6 \pi k_0^4 \sum_{m=\pm 1} S(-2mk_0, 0)\, \delta(\omega - m\omega_B) \tag{1}$$

$$\sigma^{(2)}(\omega) = 2^6 \pi k_0^4 \sum_{m_1, m_2 = \pm 1} \int\int_{-\infty}^{\infty} |\Gamma|^2 S(m_1 \mathbf{k}_1) S(m_2 \mathbf{k}_2) \times \delta(\omega - m_1\sqrt{gk_1} - m_2\sqrt{gk_2})\, dpdq \tag{2}$$

where $k_0 = (k_0, 0)$ is the absolute value of the wave number vector $\mathbf{k}_0$ of radio waves, $S(\mathbf{k}) = S(k_x, k_y)$ is the wave number spectrum of ocean surface waves and $\omega_B (= \sqrt{2gk_0})$ is the Bragg angular frequency. The independent variables, p and q, of the integration represent coordinates, each of which is parallel to the axis of the radar beam and orthogonal to the radar beam respectively. The wave number vectors for ocean waves, $\mathbf{k}_1$ and $\mathbf{k}_2$, are related to these variables by the following equations:

$$\mathbf{k}_1 = (p - k_0,\ q), \quad \mathbf{k}_2 = (-p - k_0,\ -q) \tag{3}$$

These relations indicate the Bragg's resonance condition expressed by

$$\mathbf{k}_1 + \mathbf{k}_2 = -2\mathbf{k}_0 \tag{4}$$

The coupling coefficient, Γ, shows the degree of the contribution from the wave components having the wave number $\mathbf{k}_1$ and $\mathbf{k}_2$ to the second-order energy distribution of the backscattered radar signal, and commonly expressed by $\Gamma = \Gamma_E + \Gamma_H$ [2], the summation of the electromagnetic scattering effect, Γ_E, and the hydrodynamic scattering effect, Γ_H.

Since the first-order component $\sigma^{(1)}(\omega)$ and the second-order component $\sigma^{(2)}(\omega)$ appear in different frequencies in the Doppler spectrum $\sigma(\omega)$, they can be separated; even though they are small in magnitude. Consequently, valuable oceanographic information such as surface currents and waves can be obtained from the respective spectrum components. As shown in Eq. (2), the two component waves having the wave number vector $\mathbf{k}_1$ and $\mathbf{k}_2$ are related to the second-order component $\sigma^{(2)}(\omega)$.

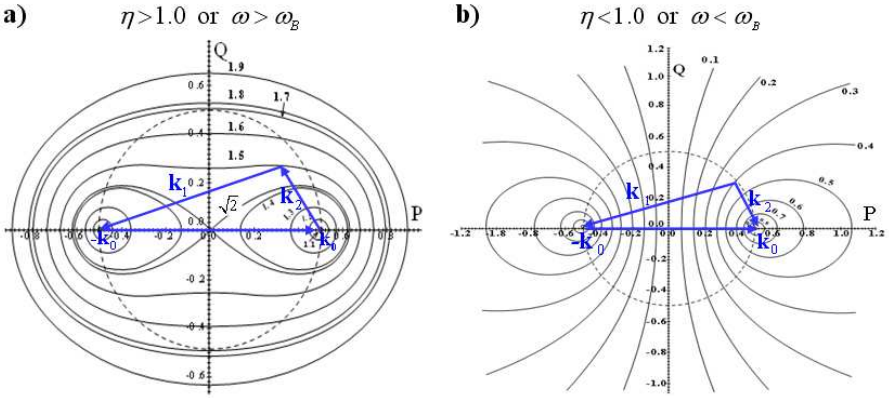

Fig. 1 Frequency contours versus wave numbers, for two wave vectors $\mathbf{k}_1$ and $\mathbf{k}_2$ producing second-order component for normalized Doppler spectrum $(\eta = \omega/\omega_B)$, a) $\eta > 1$ and b) $\eta < 1$.

The illustrations of infinite combinations of $\mathbf{k}_1$ and $\mathbf{k}_2$ which are relevant to the Doppler frequency ω under the restriction condition of δ function included in Eq. (2) and the resonance condition of Eq. (4) are shown in **Fig. 1**. As has expressed from Eq. (2), the two component waves having the wave number vector, $\mathbf{k}_1$ and $\mathbf{k}_2$, are related to the second-order scattering component $\sigma^{(2)}(\omega)$. This means that Eq. (2) includes the contributions of an infinite numbers of component waves having different frequency ω and propagation direction θ, and hence in principle, the directional spectrum can be estimated based on this information. When the directional spectrum is estimated based on Eq. (2), the following problems arise:

1) Due to the constraint of the δ function, the integration of Eq. (2) must be executed along a curve on the "frequency direction" plane into which the wave number plane is transformed by the dispersion relationship. The digitization of the integral of Eq. (2) is therefore complicated.
2) This is a so-called incomplete inverse problem in which the number of unknown parameters is much larger than that of equations obtained from the measurements. This sometimes causes the problem that even a small measurement error would seriously deteriorate the reliability of the estimate.

To estimate directional spectrum from HF radar data, it is necessary to solve a complicated two-dimensional nonlinear integral Eq. (2). Since Eq. (2) includes the contributions of infinite numbers of component waves having different frequencies ω and propagation directions θ; thus we will focus on the second-order scattering component $\sigma^{(2)}(\omega)$ and introduce a method for estimating directional wave spectra from this second-order scattering component. In this study, deep water waves have been examined. Besides, the method developed for deep water waves can be easily extended to shallow water waves.

For mathematical convenience, the parameters are non dimensionalized by the Bragg angular frequency, ω_B, and the doubled wave number of the radio wave, $2k_0$, as follows:

$$\left.\begin{array}{ll} \tilde{\omega} = \omega / \omega_B & \tilde{\mathbf{k}} = \mathbf{k} / (2k_0) \\ \tilde{\Gamma} = \Gamma / (2k_0), & \tilde{S}(\tilde{\mathbf{k}}) = (2k_0)^4 S(\mathbf{k}) \end{array}\right\} \tag{5}$$

The integration of the second-order component Eq. (2) with respect to the two variables p and q axis can be transformed into a single variable since the integrand includes the delta function δ. If the wave propagation direction θ_1 of the wave number vector $\mathbf{k}_1$ is adopted as a single independent variable for the integration, Eq. (2) can be transformed as follows [13]:

$$\tilde{\sigma}^{(2)}(\tilde{\omega}) = \int_0^{\theta_L} G(\theta_1, \tilde{\omega}) d\theta_1 \tag{6}$$

where

$$\begin{aligned} G(\theta, \tilde{\omega}) = 16\pi \Big[& |\tilde{\Gamma}|^2 \left\{ \tilde{S}(m_1 \tilde{\mathbf{k}}_1) \tilde{S}(m_2 \tilde{\mathbf{k}}_2) \right. \\ & \left. + \tilde{S}(m_1 \tilde{\mathbf{k}}_1 *) \tilde{S}(m_2 \tilde{\mathbf{k}}_2 *) \right\} y^3 \left| dy / dh \right| \Big]_{y=\hat{y}} \end{aligned} \tag{7}$$

$$\left| \frac{dy}{dh} \right| = \left| 1 + m_1 m_2 \frac{y(y^2 + \cos\theta_1)}{(y^4 + 2y^2 \cos\theta_1 + 1)^{3/4}} \right|^{-1} \tag{8}$$

and $y = \sqrt{\tilde{k}_1}$. $\hat{y}$ can be obtained by solving Eq. (9).

$$\tilde{\omega} - m_1 \hat{y} - m_2 (\hat{y}^4 + 2\hat{y}^2 \cos\theta_1 + 1)^{1/4} = 0 \tag{9}$$

$\tilde{\mathbf{k}}_i *$ is the nondimensional symmetry wave number vector of $\tilde{\mathbf{k}}_i$ with respect to the radar beam axis (the $p-$axis). An upper limit of integration can be given by $\theta_L = \pi$ when $\tilde{\omega} \le 2$, and $\theta_L = \pi - \cos^{-1}(2/\tilde{\omega}^2)$ when $\tilde{\omega} > 2$, respectively. The wave number spectrum $S(\mathbf{k})$ in Eq. (7) can be transformed into the frequency-direction spectrum (directional wave spectrum) $S(f, \theta)$ as follows:

$$S(\mathbf{k}) = \frac{g^2}{2^5 \pi^4 f^3} S(f,\theta) \tag{10}$$

Thus, by imposing the directional wave spectrum $S(f,\theta)$, the second-order component $\sigma^{(2)}(\omega)$ measured by the HF radar can be theoretically calculated by numerical integration of Eq. (6).

3. Analysis Methods for Estimating Directional Wave Spectra

A formulation and procedure to evaluate the Bayesian methods for estimating directional wave spectra from HF radar, based on Hashimoto and Tokuda[3] and Lukijanto et al[11], are presented in this section:

3.1 A Bayesian Method (BM)

In the original BM, directional spectrum is treated as a piecewise constant function with respect to each energy component of frequency and direction, including $M \times N$ unknown parameters. Here, M is the number of frequency segments, while N is the number of direction segments [3]. The problem for estimating directional wave spectrum with HF radar is to estimate a non-negative solution of $S(f,\theta)$ based on simultaneous integral equations of Eq. (6) set up for $\tilde{\sigma}^{(2)}(\tilde{\omega})$. Although, generally the directional wave spectrum is $S(f,\theta) \geq 0$, in this study, it is treated as $S(f,\theta) > 0$, and assumed to be exponential piecewise constant function over the directional range from 0 to 2π and the frequency range from $f_{\min}$ to $f_{\max}$ [14]. In addition, this assumption is commonly employed in numerically generating random waves.

$$S(f,\theta) = \alpha \sum_{i=1}^{M} \sum_{j=1}^{N} \exp(x_{i,j}) \delta_{i,j}(f,\theta) \tag{11}$$

where $x_{i,j} = \ln\{S(f_i,\theta_j)/\alpha\}$, M is the number of segments Δf of frequency f, while I is the number of segments $\Delta\theta$ of direction θ, and

$$\delta_{i,j}(f,\theta) = \begin{cases} 1: & f_{i-1} \leq f < f_i \text{ and } \theta_{j-1} \leq \theta < \theta_j \\ 0: & \text{otherwise} \end{cases} \tag{12}$$

α is a parameter introduced to normalize the magnitude of $x_{i,j}$, and given by

$$\alpha = \frac{\int_{f_{\min}}^{f_{\max}} \int_0^{2\pi} S(f,\theta)\, df d\theta}{\int_{f_{\min}}^{f_{\max}} \int_0^{2\pi} df d\theta} \tag{13}$$

The numerator on the right hand side of Eq. (13) is approximately given by the following equation[15]:

$$\int_{f_{\min}}^{f_{\max}} \int_0^{2\pi} S(f,\theta)\, df d\theta \approx \frac{2\int_{-\infty}^{\infty} \{\sigma^{(2)}(\omega)/W(\omega/\omega_B)\} d\omega}{k_0^2 \int_{-\infty}^{\infty} \sigma^{(1)}(\omega) d\omega} \tag{14}$$

where $W(\omega/\omega_B) = 8|\bar{\Gamma}^2|/k_0^2$ is a weighting function and $\bar{\Gamma}$ is an approximate coupling coefficient of Γ [15]. The frequency f and the direction θ are discretized by the following equations respectively.

$$\mu_i = \ln f_i = \ln f_{i-1} + \Delta f, \quad \theta_j = \theta_{j-1} + \Delta\theta \tag{15}$$

Substituting Eq. (11) into Eq. (6) yields an integral equation including unknown variables $M \times N$. After digitizing the Eq. (6) by replacing the integration with the summation Σ, the integral equation can be approximated by the nonlinear algebraic equation. However, it is unrealistic to assume that the energy distribution over wave frequency f and wave propagation direction θ can be discontinuous. Thus, $S(f,\theta)$ is generally considered to be a continuous and smooth function.

The integral of Eq. (6) is, however, a curvilinear integral where the integration must be performed along a special path in $(f,\ \theta)$ plane due to the restrictions of Eqs. (4) and (9). As mentioned earlier, Eq. (6) includes a singular point, and has to be integrated with smaller segments around the singular point. In discretizing Eq. (6), the value of the directional wave spectrum along the path in $(f,\ \theta)$ plane is linearly interpolated by the neighboring grid point values of the directional wave spectrum in the same way as Hisaki [6], and expressed by

$$\begin{aligned} S(\mu,\theta) = {} & (1-\xi)\ S(\mu_i,\theta) + \xi\ S(\mu_{i+1},\theta) \\ & + (1-\xi)\ \zeta\ S(\mu_i,\theta_{j+1}) + \xi\ \zeta\ S(\mu_{i+1},\theta_{j+1}) \end{aligned} \tag{16}$$

where $\mu = \ln f$, $0 \le \xi$ and $\zeta \le 1$. Eq. (6) can therefore be digitized with respect to the grid point values of $S(\mu_i,\theta_j)$ with the desired degree of accuracy.

Finally, by taking into account the errors ε_k of the Doppler spectrum, the integral Eq. (6) can be approximated by the nonlinear algebraic equation including the unknown $\mathbf{X} = (x_{1,1},\cdots,x_{I,J})^t$, and expressed by:

$$\tilde{\sigma}_k^{(2)} = F_k(\mathbf{X}) + \varepsilon_k \tag{17}$$

where the suffix k indicates a value of the Doppler frequency $\tilde{\omega}_k$ $(k = 1,\cdots,K)$. The errors ε_k $(k = 1,\cdots,K)$ of every Doppler frequency $\tilde{\omega}_k$ are assumed to be independent of each other and their occurrence probabilities can be expressed by a normal distribution having a zero mean and variance λ^2. Then, for a given $\tilde{\sigma}_k^{(2)}(k = 1,\cdots,K)$, the likelihood functions of $\mathbf{X}$ and λ^2 is given by:

$$L(\mathbf{X};\lambda^2) = \frac{1}{(\sqrt{2\pi}\lambda)^K} \exp\left[-\frac{1}{2\lambda^2} \sum_{k=1}^{K} \left\{ \tilde{\sigma}_k^{(2)} - F_k(\mathbf{X}) \right\}^2 \right] \tag{18}$$

It should be noted that the directional wave spectrum $S(f,\theta)$ has thus far been expressed by a piecewise constant function, with the correlation between the wave energy of each segment of $\Delta f \times \Delta\theta$ not yet having been taken into account. As directional wave analysis is commonly based on the linear wave theory, it can be assumed that each of energy on each segment is independent of each other. In general, $S(f,\theta)$ is considered to be a continuous and smooth function. This allows an introduction of an additional condition that the local variation of $x_{i,j}$ $(i = 1,\cdots,I;\ j = 1,\cdots,J)$ can be well approximated by a smooth surface so that the value given in Eq. (19) is expected to be small [14].

$$x_{i,j+1} + x_{i+1,j} + x_{i,j-1} + x_{i-1,j} - 4x_{i,j} \tag{19}$$

In the upper boundary ($i = I$) and the lower boundary ($i = 1$) of the frequency f , the value given in Eq. (20) is expected to be small as a priori condition.

$$x_{i,j+1} - 2x_{i,j} + x_{i,j-1} \tag{20}$$

These additional conditions lead to

$$\begin{aligned} &\sum_{i=2}^{I-1}\sum_{j}(x_{i,j+1} + x_{i+1,j} + x_{i,j-1} + x_{i-1,j} - 4x_{i,j})^2 \\ &\quad + \sum_{j}(x_{1,j+1} - 2x_{1,j} + x_{1,j-1})^2 + \sum_{j}(x_{I,j+1} - 2x_{I,j} + x_{I,j-1})^2 \ \rightarrow \ \text{small} \end{aligned} \tag{21}$$

(where $x_{i,0} = x_{i,J}$, $x_{i,-1} = x_{i,J-1}$)

From algebraic viewpoint, Eq. (21) can be written in the matrix form, as

$$\| \mathbf{DX} \|^2 \tag{22}$$

where $\mathbf{D}$ is the coefficient matrix of Eq. (21). It is, therefore, surmised that the optimal estimate of $S(f,\theta)$ is the one maximizing the likelihood function of Eq. (18) under the condition of Eq. (22). More precisely, the most suitable estimate is given as a set of $\mathbf{X} = (x_{1,1}, \cdots, x_{I,J})^t$ which maximizes the following equation for a given hyperparameter u^2 .

$$\ln L(\mathbf{X}; \lambda^2) - \frac{u^2}{2\lambda^2} \| \mathbf{DX} \|^2 \tag{23}$$

The hyperparameter u^2 is a type of weighting coefficient which represents the smoothness of $\mathbf{X}$, where large or small values of u , respectively, give an estimate of the directional wave spectrum having either smooth or rough shapes. It should be noted that Eq. (23) corresponds to the Bayesian relationship expressed by the following equation when we consider the exponential function with the power of Eq. (23).

$$p_{\mathrm{POST}}(\mathbf{X} \mid u^2, \lambda^2) = L(\mathbf{X}; \lambda^2)\, p(\mathbf{X} \mid u^2, \lambda^2) \tag{24}$$

where $p_{\mathrm{POST}}(\mathbf{X} \mid u^2, \lambda^2)$ the posterior distribution, and $p(\mathbf{X} \mid u^2, \lambda^2)$ the prior distribution of $\mathbf{X} = (x_{1,1}, \cdots, x_{I,J})^t$ expressed by

$$p(\mathbf{X} \mid u^2, \lambda^2) = \left(\frac{u}{\sqrt{2\pi}\lambda} \right)^{I \times J} \exp\left\{ -\frac{u^2}{2\lambda^2} \| \mathbf{DX} \|^2 \right\} \tag{25}$$

The estimate $\mathbf{X}$ obtained by maximizing Eq. (23) can be considered as the mode of the posterior distribution $p_{\mathrm{POST}}(\mathbf{X} \mid u^2, \lambda^2)$. Now, if the value of u is given, then regardless the value of λ^2 , the values of $\mathbf{X}$ that maximize Eq. (23) can be determined by minimizing

$$\sum_{k=1}^{K}\left\{ \tilde{\sigma}_k^{(2)} - F_k(\mathbf{X})\right\}^2 + u^2 \| \mathbf{DX} \|^2 \tag{26}$$

Eventually, from the view point of the suitability and smoothness of the $\mathbf{X}$ estimation, the determination of u and the estimation of λ^2 can be automatically performed by minimizing the following ABIC (Akaike's Bayesian Information Criterion)[16]:

$$\mathrm{ABIC} = -2\ln \int L(\mathbf{X} \mid \lambda^2)\, p(\mathbf{X} \mid u^2, \lambda^2) d\mathbf{X} \tag{27}$$

3.2 A Modified Bayesian Method (MBM)

The major distinct modifications are described in this section which focuses to reduce the computation time by modifying the formulation of the directional spectrum and the procedure of iterative computation. Here, with regards to the $S(f,\theta)$ in Eq. (10), a new formulation of function expressed by Eq. (28) was developed by introducing a similar formulation of Maximum Entropy Principle (MEP) described by Hashimoto and Kobune[12]. The determination of the directional wave spectrum from HF radar can then be achieved by the inversion of Eq. (6) using the similar way as described by Hashimoto and Tokuda[3]. From this point of view, Lukijanto et al[11] expanded the directional wave spectrum function, as an exponential function having the power expressed by a Fourier series over the direction while piecewise constant function over the frequency:

$$S(f_i,\theta) = \exp\left[a_0(f_i) + \sum_{k=1}^{K}\left\{ a_k(f_i)\cos k\theta + b_k(f_i)\sin k\theta \right\}\right] \tag{28}$$

where f_i is wave frequency discretized by the Eq. (15), meanwhile $a_k(f_i)$ and $b_k(f_i)$ are unknown coefficients to be estimated.

In this case, M is assumed to be the number of frequency segments and K is the number of Fourier series, and then the number of unknown coefficients becomes $M \times (2K+1)$. Hashimoto and Kobune[12] explained that although the number of Fourier series used $K=1$, not only the narrow single peak directional spectrum, but also very wide energy distribution was accurately shown. Substituting Eq. (28) into Eq. (6) yields an integral equation including unknown coefficients $a_k(f_i)$ and $b_k(f_i)$. Here, fine segment around the singular point is necessarily adopted to have accurate calculation. Similar way to the BM, the integration must be performed along a path in (f,θ) plane as described in section 2, due to the restriction condition of δ function included in Eq. (2). Afterwards, Eq. (6) can be digitized with respect to the grid point values of $S(\mu_i,\theta_j)$ described in Eq. (16). Then, by taking into account the errors ε_l of Doppler spectrum, the integral of Eq. (6) can be approximated by non linear algebraic governing equation including the unknown variable $\mathbf{X}=\left[a_0(f_i), a_k(f_i) \,\&\, b_k(f_i);\ i=1,...,M,\ k=1,...,k\right]$, which is expressed and corresponds to the Eq. (17). Moreover, the likelihood functions of $\mathbf{X}$ and λ^2 is also given by similar to Eq. (18).

Although different assumption of the energy distribution over propagation direction was applied to the MBM, each component in frequency still remains discontinuous. However, $S(f,\theta)$ is generally considered to be a continuous and smooth function in both frequency and direction.

This allows an introduction of additional conditions that the coefficients of $a_k(f_i)$ and $b_k(f_i)$ in Eq. (28) are locally continuous between adjacent frequencies in directional spectrum $S(f,\theta)$. Hence, the following values can be assumed to be small:

$$\left.\begin{array}{l} a_k(f_{i+1}) - 2a_k(f_i) + a_k(f_{i-1}) \rightarrow \text{small} \\ b_k(f_{i+1}) - 2b_k(f_i) + b_k(f_{i-1}) \rightarrow \text{small} \end{array}\right\} \tag{29}$$

Under this assumption, Eq. (29) is not valid for the lower limit $(i=1)$ and the upper limit $(i=M)$ of frequency *f*, In this case, $a_k(f_i)$ and $b_k(f_i)$ become a type of boundary conditions. Therefore, these boundary conditions have to be properly given. However, it is difficult to give those values in advance before the estimation. Alternatively, other assumption may be applied to give the boundary values.

When the order of the Fourier series in Eq. (28) is K, then the number of unknown parameters becomes $M\times(2K+1)$, and the equation assumed in Eq. (29) will be $(M-2)\times(2K+1)$, while the number of fundamental equation with respect to the second order component $\sigma^{(2)}(\omega)$ is *L*. Thus, under the condition of $L+(M-2)\times(2K+1)\geq M\times(2K+1)$, the boundary parameters of $a_k(f_1)$ and $b_k(f_1)$, $a_k(f_M)$ and $b_k(f_M)$ may automatically be estimated using the least squares method. Unfortunately based on our investigations, this method sometimes causes unstable estimation of the coefficient $a_k(f_i)$ and $b_k(f_i)$. For convenience; therefore the following conditions are assumed to be small at the boundary frequency of $i=1$ and M :

$$\left.\begin{array}{l} a_k(f_{i+1}) - a_k(f_i) \rightarrow \text{small} \\ b_k(f_{i+1}) - b_k(f_i) \rightarrow \text{small} \end{array}\right\} \tag{30}$$

These conditions impose a small energy change between the adjacent frequencies at the boundary frequencies. In the following, an operational matrix **D** is introduced for convenience. **D** is an operational matrix which expresses the condition of Eqs. (29) and (30). Therefore, if the value obtained by $\|\mathbf{DX}\|^2$ is small, the results of directional spectrum estimation appear to be smooth. Thus, it is supposed that the optimal estimate of $S(f,\theta)$ is the one that maximizing the likelihood function of Eq. (18) under the condition of Eq. (22) in the same way as BM. More precisely, the most suitable estimate is given as a set of $\mathbf{X}=[a_k(f_i)\,\&\,b_k(f_i)]^t$ which maximizes the equation for a given hyperparameter u^2 as shown in Eq (23). Based on the posterior distribution as defined in Eq. (24), the prior distribution of $\mathbf{X}$ can be expressed as follows:

$$p(\mathbf{X}\,|\,u^2,\lambda^2) = \left(\frac{u}{\sqrt{2\pi}\lambda}\right)^{M\times(2K+1)} \exp\left\{-\frac{u^2}{2\lambda^2}\|\mathbf{DX}\|^2\right\} \tag{31}$$

The estimate $\mathbf{X}$ obtained by maximizing Eq. (23) can be considered as the mode of the posterior distribution $p_{\mathrm{POST}}(\mathbf{X}\,|\,u^2,\lambda^2)$. Now, if the value of u is given, regardless of the value of λ^2, the values of $\mathbf{X}$ that maximize Eq. (23) can be determined by minimizing:

$$\sum_{l=1}^{L}\left\{\tilde{\sigma}_l^{(2)} - F_l(\mathbf{X})\right\}^2 + u^2\,\|\mathbf{DX}\|^2 \tag{32}$$

Moreover, by minimizing the ABIC in Eq. (27), the determination of u and the estimation of λ^2 can be automatically deduced also. Based on the above analysis, we can summarize that the inversion problem of the BM and MBM are literally similar in methodological sequences. The detail numerical calculations as well as the discussions of some ideas for improving them are briefly described in the following sections.

4. Numerical Computation Procedures

4.1 Linearization of Equations to be Solved

This section provides computational information about the two developed techniques. Before doing this, an overview of the numerical computations will be presented and important features of the procedures will be highlighted. Numerical computations were conducted to estimate the directional wave spectrum using the BM which requires minimization of Eqs. (26) and (27); the similar procedure is applied to the MBM for Eqs. (32) and (27). However, it is impossible to carry out them analytically.

Since the first term on the right-hand side of Eq. (17) is nonlinear with respect to $\mathbf{X}$, it is linearized using Taylor expansion around $\mathbf{X}_0$, having value close to estimate solution of $\mathbf{X}=\left[x_{1,1},...,x_{I,J}\right]^t$ and $\mathbf{X}=\left[a_k\left(f_i\right)\&\, b_k\left(f_i\right)\right]^t$ for the BM and MBM respectively. It can be written as:

$$F_k(\mathbf{X}) = F_k\left(\mathbf{X}_0\right) + G_k\left(\mathbf{X}_0\right)\left(\mathbf{X}-\mathbf{X}_0\right) \tag{33}$$

in which:

$$\mathbf{G}_k(\mathbf{X}_0) = \left[\ \partial F(\mathbf{X})/\partial x_{1,1}, \cdots, \partial F(\mathbf{X})/\partial x_{I,J}\ \right]_{\mathbf{X}=\mathbf{X}_0} \tag{34}$$

Substitution of Eq. (33) into Eq. (17) and rearrangement in the matrix form give the following linearized equation with respect to the $\mathbf{X}$.

$$\mathbf{B} = \mathbf{A}\mathbf{X} + \mathbf{E} \tag{35}$$

where

$$\begin{aligned} &\mathbf{A} = \left[\mathbf{G}_1(\mathbf{X}_0), \cdots, \mathbf{G}_K(\mathbf{X}_0)\right], \qquad \mathbf{E} = \left[\varepsilon_1, \cdots, \varepsilon_K\right]^t, \\ &\mathbf{B} = \left[\tilde{\sigma}_1^{(2)} - F_1(\mathbf{X}_0) + \mathbf{G}_1(\mathbf{X}_0)\mathbf{X}_0, \cdots, \tilde{\sigma}_K^{(2)} - F_K(\mathbf{X}_0) + \mathbf{G}_K(\mathbf{X}_0)\mathbf{X}_0\right]^t \end{aligned} \tag{36}$$

Therefore, the Eq. (26) and Eq. (32) for the BM and MBM respectively, become:

$$W(\mathbf{X}) = \| \mathbf{A}\mathbf{X} - \mathbf{B} \|^2 + u^2 \| \mathbf{D}\mathbf{X} \|^2 \tag{37}$$

4.2 Some Modifications for Improving Iterative Computation

The initial value has been modified to minimize Eq. (37). As described in Hashimoto and Tokuda[3], for given u in Eq. (37) and Eq. (27) in our numerical methods, the optimum value $\hat{\mathbf{X}}$

can be estimated by the least-squares method. However, particularly for the MBM, different expression has been possibly proposed for Eq. (33) by modifying Eqs. (29) and (30). That is, an alternative expression is introduced by introducing $\Delta\mathbf{X} = \mathbf{X} - \mathbf{X}_0$. Then, another form of Eq. (33) is redefined and expressed as:

$$F_k(\mathbf{X}) = F_k(\mathbf{X}_0) + G_k(\mathbf{X}_0)\Delta\mathbf{X} \tag{38}$$

In this case $\mathbf{B}$ is defined as $\mathbf{B} = \left[\tilde{\sigma}_1^{(2)} - F_1(\mathbf{X}_0), ..., \tilde{\sigma}_K^{(2)} - F_K(\mathbf{X}_0)\right]^t$ and Eq. (35) becomes $\mathbf{B} = \mathbf{A}\Delta\mathbf{X} + \mathbf{E}$. This is the linear equation with respect to the $\Delta\mathbf{X}$. Therefore, the alternative additional conditions for Eqs. (29) and (30) may be used with respect to the $\Delta\mathbf{X}$:

$$\left.\begin{array}{l} \Delta a_k(f_{i+1}) - 2\Delta a_k(f_i) + \Delta a_k(f_{i-1}) \rightarrow \text{small} \\ \Delta b_k(f_{i+1}) - 2\Delta b_k(f_i) + \Delta b_k(f_{i-1}) \rightarrow \text{small} \\ (i = 2, ..., M-1) \end{array}\right\} \text{ and } \left\{\begin{array}{l} \Delta a_k(f_{i+1}) - 2\Delta a_k(f_i) \rightarrow \text{small} \\ \Delta b_k(f_{i+1}) - 2\Delta b_k(f_i) \rightarrow \text{small} \\ (i = 1 \ \ and \ \ M) \end{array}\right\}$$

Note that after rearrangement, a new matrix form can be deduced as:

$$W(\Delta\mathbf{X}) = \| \mathbf{A}\Delta\mathbf{X} - \mathbf{B} \|^2 + u^2 \| \mathbf{D}\Delta\mathbf{X} \|^2 \tag{39}$$

Eqs. (37) and (39) seems to be very similar except unknown variable $\mathbf{X}$ and $\Delta\mathbf{X}$. Actually, the first term in the right hand side of the both equations are same. However, the minimization of the second terms in each of Eqs. (37) and (39) has different meaning. That is, although the minimization of the second term in Eq. (37) expects the smoothness and the continuance of the directional spectrum itself. Meanwhile, the one in Eq. (39) expects the smoothness and continuance of the difference of the directional spectrum between the successive iterative computations. The success of this modified method with Eq. (39) was described in Lukijanto et al[11].

4.3 Estimation Procedures for a General Data Set

According to Hashimoto[10], the least-square method is carried out for Eqs. (37) and (39) via Householder transformation by transforming a matrix to an upper triangular matrix by repeating a mirror image transformation as follows.

Although, the following procedures are explained for the minimization of Eq. (37) of BM, $\mathbf{X}$ is to be replaced by $\Delta\mathbf{X}$ for the minimization of Eq. (39) of MBM. Then, Eq. (37) can be rewritten as:

$$W(x) = \left\| \begin{pmatrix} \mathbf{A} \\ u\mathbf{D} \end{pmatrix} \mathbf{X} - \begin{pmatrix} \mathbf{B} \\ 0 \end{pmatrix} \right\|^2 \tag{40}$$

For convenience, the following matrix is assumed:

$$\mathbf{Z} = \begin{bmatrix} \mathbf{A} & \mathbf{B} \\ u\mathbf{D} & 0 \end{bmatrix} \tag{41}$$

Afterward, the Householder transformation is applied such that the following matrix is obtained:

$$\mathbf{UZ} = \begin{bmatrix} \begin{pmatrix} S_{1,l} & \cdots & S_{1,K+1} \\ & \ddots & \vdots \\ 0 & \cdots & S_{K+1,K+1} \end{pmatrix} \end{bmatrix} \tag{42}$$

where **U** denoted the transformation operator. Eq. (40) can then be rewritten as:

$$\left\| \mathbf{U}\begin{pmatrix} \mathbf{A} \\ u\mathbf{D} \end{pmatrix}\mathbf{X} - \mathbf{U}\begin{pmatrix} \mathbf{B} \\ 0 \end{pmatrix} \right\|^2 = \left\| \begin{pmatrix} S_{1,l} & \cdots & S_{1,K} \\ & \ddots & \vdots \\ 0 & \cdots & S_{K,K} \end{pmatrix} \begin{pmatrix} \mathbf{X}_1 \\ \vdots \\ \mathbf{X}_K \end{pmatrix} - \begin{pmatrix} S_{1,K+1} \\ \vdots \\ S_{K+1,K+1} \end{pmatrix} \right\|^2$$

$$= \left\| \begin{pmatrix} S_{1,1} & \cdots & S_{1,K} \\ & \ddots & \vdots \\ 0 & \cdots & S_{K,K} \end{pmatrix} \begin{pmatrix} \mathbf{X}_1 \\ \vdots \\ \mathbf{X}_K \end{pmatrix} - \begin{pmatrix} S_{1,K+1} \\ \vdots \\ S_{K,K+1} \end{pmatrix} \right\|^2 + S_{K+1,K+1}^2 \tag{43}$$

As the second term of the right hand-side of Eq. (43) is independent of $\mathbf{X}$, the estimate of $\hat{\mathbf{X}}$ which minimizes Eqs. (39) or (40), is obtained by solving Eq. (44).

$$\begin{pmatrix} S_{1,1} & \cdots & S_{1,K} \\ & \ddots & \vdots \\ 0 & \cdots & S_{K,K} \end{pmatrix} \begin{pmatrix} \mathbf{X}_1 \\ \vdots \\ \mathbf{X}_K \end{pmatrix} = \begin{pmatrix} S_{1,K+1} \\ \vdots \\ S_{K,K+1} \end{pmatrix} \tag{44}$$

The estimate variance of the residual, $\hat{\sigma}^2$, in Eq. (39), is calculated by using

$$\hat{\sigma}^2 = S^2{}_{K+1,K+1} / (2N) \tag{45}$$

Thus, the ABIC (Eq. 27) can now be calculated. By denoting $\hat{\mathbf{A}}$ and $\hat{\mathbf{B}}$ as the final coefficient matrices $\mathbf{A}$ and $\mathbf{B}$ used to determine estimate $\hat{\mathbf{X}}$, the right-hand side of the posterior distribution Eq. (24) can be expressed as:

$$\begin{aligned} & L(x,\sigma^2)\, p(x \mid u^2,\sigma^2) \\ & \approx \left(\frac{1}{2\pi\sigma^2}\right)^N \exp\left\{-\frac{1}{2\sigma^2}\left\|\hat{\mathbf{A}}\mathbf{X}-\hat{\mathbf{B}}\right\|^2\right\}\left(\frac{u}{\sqrt{2\pi\sigma}}\right)^K \exp\left\{-\frac{u^2}{2\sigma^2}\|\mathbf{D}\mathbf{X}\|^2\right\} \\ & = \left(\frac{1}{2\pi\sigma^2}\right)^N \left(\frac{u}{\sqrt{2\pi\sigma}}\right)^K \exp\left\{-\frac{1}{2\sigma^2}\left\|\begin{pmatrix}\hat{\mathbf{A}}\\ u\mathbf{D}\end{pmatrix}\hat{\mathbf{X}}-\begin{pmatrix}\hat{\mathbf{B}}\\ 0\end{pmatrix}\right\|^2\right\} \times \exp\left\{-\frac{1}{2\sigma^2}\left\|\begin{pmatrix}\hat{\mathbf{A}}\\ u\mathbf{D}\end{pmatrix}(\mathbf{X}-\hat{\mathbf{X}})\right\|^2\right\} \end{aligned} \tag{46}$$

Applying

$$\int_{-\infty}^{\infty} \exp\left\{-\frac{1}{2\sigma^2}\left\|\begin{pmatrix}\hat{\mathbf{A}}\\ u\mathbf{D}\end{pmatrix}(\mathbf{X}-\hat{\mathbf{X}})\right\|^2\right\}dx$$
$$=\left(\sqrt{2\pi\sigma}\right)^K\left\{\det\left(\hat{\mathbf{A}}^t\hat{\mathbf{A}}+u^2\mathbf{D}^t\mathbf{D}\right)\right\}^{-\frac{1}{2}} \tag{47}$$

and integrating both side of Eq. (46) with respect to $\mathbf{X}$ gives

$$\int_{-\infty}^{\infty} L\left(x,\sigma^2\right)p\left(x\middle|u^2,\sigma^2\right)dx$$
$$=\left(\frac{1}{2\pi\sigma}\right)^N u^K\exp\left[-\frac{1}{2\sigma^2}\left\{\left\|\hat{\mathbf{A}}\hat{\mathbf{X}}-\hat{\mathbf{B}}\right\|^2+u^2\left\|\mathbf{D}\hat{\mathbf{X}}\right\|^2\right\}\right]\left\{\det\left(\hat{\mathbf{A}}^t\hat{\mathbf{A}}^t+u^2\mathbf{D}^t\mathbf{D}\right)\right\}^{-1/2} \tag{48}$$

From these results, the ABIC given in Eq.(27) becomes

$$\begin{aligned}\mathrm{ABIC} &= -2\ln\int_{-\infty}^{\infty} L\left(x,\sigma^2\right)p\left(x\middle|u^2,\sigma^2\right)dx\\ &= 2N\ln\left(2\pi\sigma^2\right)-K\ln\left(u^2\right)+\frac{1}{\sigma^2}\left\{\left\|\hat{\mathbf{A}}\hat{\mathbf{X}}-\hat{\mathbf{B}}\right\|^2+u^2\left\|\mathbf{D}\hat{\mathbf{X}}\right\|^2\right\}+\ln\left\{\det\left(\hat{\mathbf{A}}^t\hat{\mathbf{A}}+u^2\mathbf{D}^t\mathbf{D}\right)\right\}\end{aligned} \tag{49}$$

The estimate of the variance (σ^2) which minimizes the ABIC is obtained by solving:

$$\frac{\partial(\mathrm{ABIC})}{\partial\sigma^2}=\frac{2N}{\sigma^2}-\frac{1}{\sigma^4}\left\{\left\|\hat{\mathbf{A}}\hat{\mathbf{X}}-\hat{\mathbf{B}}\right\|^2+u^2\left\|\mathbf{D}\hat{\mathbf{X}}\right\|^2\right\}=0 \tag{50}$$

with the solution being the optimal estimate of σ^2 minimizing the ABIC. Thus, the estimate $\hat{\sigma}^2$ is

$$\hat{\sigma}^2=\frac{1}{2N}\left\{\left\|\hat{\mathbf{A}}\hat{\mathbf{X}}-\hat{\mathbf{B}}\right\|^2+u^2\left\|\mathbf{D}\hat{\mathbf{X}}\right\|^2\right\} \tag{51}$$

Finally, the resultant ABIC is obtained as

$$\mathrm{ABIC}=2N\left\{\ln\left(2\pi\hat{\sigma}^2\right)+1\right\}-K\ln\left(u^2\right)+\ln\left\{\det\left(\hat{\mathbf{A}}^t\hat{\mathbf{A}}+u^2\mathbf{D}^t\mathbf{D}\right)\right\} \tag{52}$$

Note that Eqs. (51) and (45) are identical. In the computation of the ABIC, those are also necessary to perform the calculation of the determinant of the matrix in the last term of Eq. (52). If the last term on the right-hand side of Eq. (52) is directly calculated using a conventional matrix computation method, obtaining the ABIC is often impossible due to the floating-point exception rule utilized in digital computers. Consequently, we use:

$$\ln\left\{\det\left(\hat{\mathbf{A}}^t\hat{\mathbf{A}}+u^2\mathbf{D}^t\mathbf{D}\right)\right\}=\sum_{i=1}^{K}\ln S_{i,i}^2 \tag{53}$$

where $S_{i,i}$ denotes the diagonal element of the coefficient matrix Eq. (42). The optimal hyperparameter *u* that minimizes the ABIC is determined via trial and error by changing *m* in the following equation.

$$u = ab^m \quad (m = 1, 2, ...) \tag{54}$$

where a and b are the search coefficients, according to the Hashimoto and Tokuda[3], here chosen for the convenience as $a = 0.1$ and $b = 0.5$. Finally, the whole procedure mentioned in this section is summarized as follows:

1. For a value of the hyperparameter u given by Eq. (54) and the initial value $\mathbf{X}_0 \left(\mathbf{X}_i = 0; \left(i = 1, ..., K \right) \right)$, compute $\hat{\mathbf{X}}$ using the least-squares method to iteratively minimize Eq. (39). That is, for $\mathbf{X}_0$, a new value $\mathbf{X}_1$ is obtained by applying the least-squares method.
2. Then by replacing $\mathbf{X}_0$, Eq. (37) is terminated when the standard deviation of the difference $\mathbf{X}$ values in two successive steps is less than 10^{-3}. The iteration of this process continues until $\mathbf{X}$ converges to $\hat{\mathbf{X}}$ for the given u.
3. Use the given $\hat{\mathbf{X}}$, u and Eq. (51) to determine (σ^2), and then compute the ABIC in Eq. (52).
4. After changing the value of u given by Eq. (54), then repeat the process of 1) and 2). For brevity, from various estimates of $\hat{\mathbf{X}}$ obtained through the process 1) through 3), select the values $\hat{u}^2$ and $\hat{\sigma}^2$, as well as $\hat{\mathbf{X}}$ which yields the minimum ABIC.

4.4 Examination of the BM and MBM by Numerical Simulation

For the purpose to compare the performance of the two methods, i.e. BM and MBM, the numerical simulations have been tested upon: ability to estimate correctly, robustness and reliability of results. Subsequently, the equation containing unknown parameters $M \times N$ is needed to solve in the case of BM in which M and N are the number of the frequency and the directional segments respectively. For practical convenience to limit computation time processing, basically the too large number of segments can not be set. Based on the computational efficiency, the validity and accuracy of the methods are qualitatively compared. Therefore, the time taken to do this computation is the limiting factor for the practical analysis as described in Secs. 4.1- 4.3.

Figure 2 shows the results of numerical simulation using BM. Two types of bi-directional wave field are assumed where dominant energy peaks of the directional wave spectrum are assumed to be in: (**a**) different frequencies, and (**b**) the same frequencies. The benchmark (true) of directional wave spectra is drawn at upper panel left side whereas the estimated one is drawn underneath the benchmark (true) of directional wave spectra. The middle and the right panel of each figure show the frequency spectrum $S(f)$ and the directional distribution function $G(\theta)$ in the frequency $f = 0.093$(Hz) of the directional spectrum respectively. Each directional wave spectrum was estimated from the two Doppler spectra which frequency of the radar and the crossing angle of radio signals $(\delta\theta)$ were assumed to be 24.515 MHz and 75° respectively. The significant wave period $T_{1/3}$ of 5 and 12 seconds are also assumed for **Fig. 2.a** and 10 second for **Fig. 2.b**. The thin lines represent the true frequency spectrum and directional distribution function. While the thick lines represent the estimation.

The result shows that the estimated directional wave spectrum by using BM is qualitatively good agreement with the true one. As shown in **Fig. 2.a**, the estimated frequency spectrum is underestimated around the energy peak. Although the estimated directional distribution function is overestimated around the energy peak, the locations of energy peaks of the estimated frequency spectrum and the estimated directional distribution function are properly estimated.

Figures 2.b shows that the estimated directional wave spectrum and directional distribution function perform similar trend with that assumed to be in different frequencies (**Fig. 2.a)**. However, the estimated frequency spectrum is underestimated around the energy peak. From the numerical simulation, we concluded that the BM has demonstrated to be a stable and reliable method for estimating directional wave spectra from Doppler spectra. However, the disadvantage of BM is a time consuming method related to the matrix calculation of Eq. (37) as discussed in Secs. 3 and 4. Thus great computational efforts have to be taken into account.

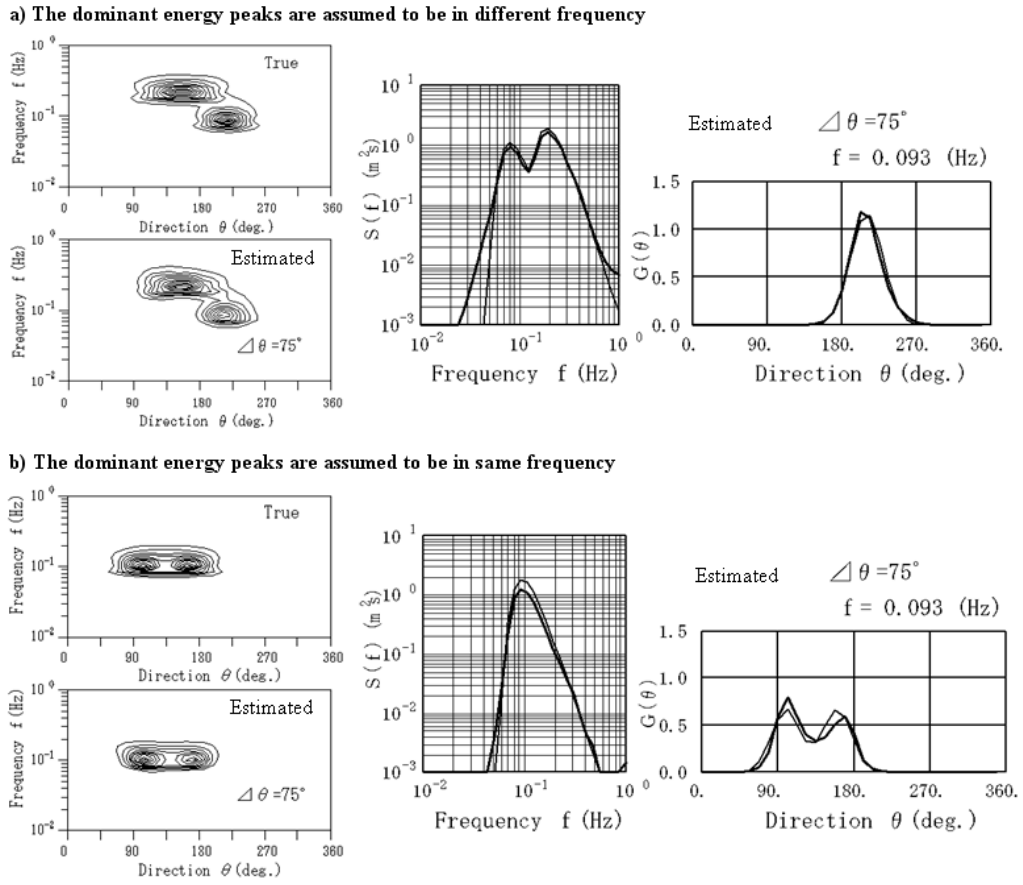

Fig. 2. The directional wave spectra estimated by using Bayesian Method (BM) where the dominant energy peaks of directional wave spectra are assumed to be in (a) different frequency and (b) same frequency at the different crossing angle (75°) of two beam axes (described by Hashimoto and Tokuda[3]). The thin lines represent the true frequency spectrum $S(f)$ and directional distribution function $G(\theta)$. While the thick lines represent the estimation ones.

In order to verify effect of the modifications described in section 3.2, extensive tests were done to analyze the accuracy and applicability of the MBM compared to the previous BM. **Figure 3** shows bi-directional wave field calculated by MBM using Eq. (39). The same conditions are set to be equal to those of **Fig. 2**.

The results show that the estimated directional wave spectrum is qualitatively good agreement with the true directional wave spectra. The estimated frequency spectrum is underestimated around the energy peak. However, the slight excessive energy was estimated at the lower frequency side. The numerical result where dominant energy peaks of the directional wave spectrum are assumed to be in different frequencies (**Fig. 3.a**) shows that the estimated frequency spectra perform good

enough with those assumed to be in the same frequencies (**Fig. 3.b**). Although the estimated directional distribution function shows a little inconsistency results, the estimation accuracy is acceptable in practical application.

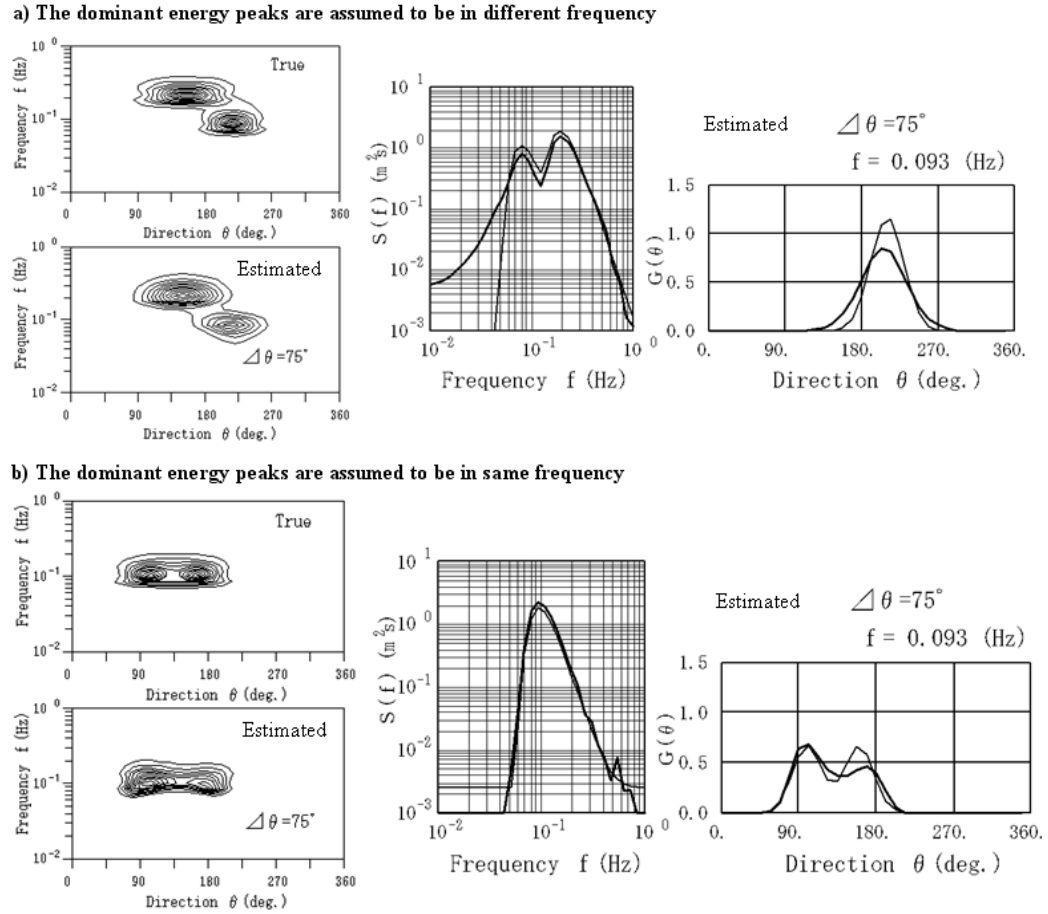

Fig. 3. As for **Fig**. **2** but estimated using MBM described by Lukijanto et al[11].

Based on the results, the BM and MBM have suggested that there are reasonable agreements between the true and estimated directional wave spectra in terms of the energy spectrum, as illustrated in **Figs. 2** and **3**. In addition, in the estimation of the directional spectrum using a BM, a normal personal computer takes tens of seconds to compute the directional spectrum even in the case of M=N=16. Meanwhile, in the case of M=N=32, it takes several minutes to compute which is presently impractical for real-time processing. In order to reduce the computation time, the MBM is subsequently applied. The results showed that an enormous amount of computation time can be reduced by using MBM. The estimation of the directional spectrum was obtained within several seconds. This computation time demonstrates 10 to 100 times faster than using BM, which is permissible for practical use. Having such properties, the MBM are capable of executing the high speed computing and consequently possible to reduce memory required for computations. The important point can be suggested that the MBM performs more efficient than the BM. Accordingly, the MBM has a good potential for operational application.

From the abovementioned explanation, the MBM may turn out to be not only accurate and reliable but also practical method for estimating directional wave spectra from HF radar.

Additionally, in the following section the accuracy and suitability of both methods, the BM and MBM, will be verified with actual field data obtained from the SCAWVEX project.

5. Verification of Applicability of MBM with SCAWVEX`s Data

5.1 SCAWVEX Project

The data set was collected by the Surface Current and Wave Variability Experiments (SCAWVEX) project with the data quality considered to be reliable enough and confirmed[17]. For that reason, these data were selected to demonstrate the validity of the BM and MBM. In this project, advancing coastal HF radar applications was one of the objectives of SCAWVEX.

Observations by these HF radars were made at the two sites at Holderness in the United of Kingdom (UK) located on the east coast of the UK and facing the North Sea shown in **Fig. 4**. The observed points A to I are indicated for which directional wave spectra will be computed by using BM and MBM. The stripe symbol denoted by Master and Slave shows the locations of HF radar points, whereas the white circles represent the Doppler spectra measurements points. These observations were carried out from December 1995 to January 1996.

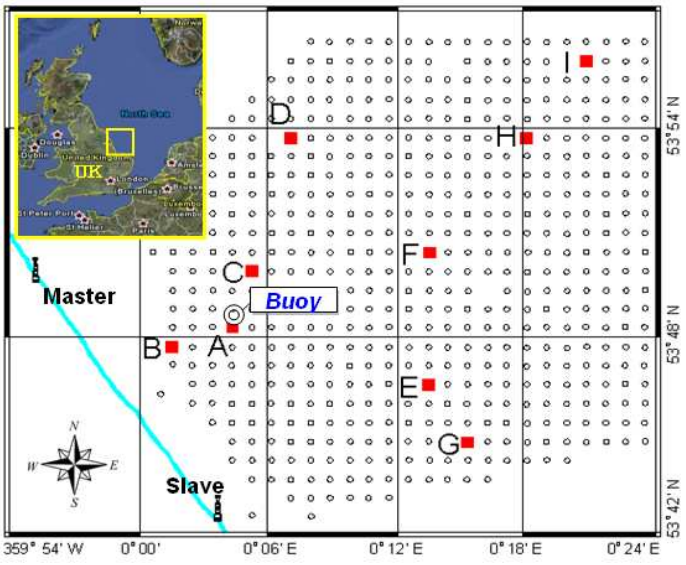

Fig. 4. Position of HF ocean radar systems at Master and Slave (UK) and the wave buoy deployment. The observed points A to I are indicated for which directional wave spectra analyzed by BM and MBM.

The observation data obtained at 14:00 on December 21, 1995, are used where the bi-directional wave fields were formed at 00:00. As reported by Hashimoto et al[5], before and after this date, the low-pressure system was stationary in the sea area west of the UK. Wyatt[18] explained also that during that date, swell dominating over most of the region propagating from north and refracting toward coast occurred. To the south, south-easterly wind waves dominate. In addition to the HF radar systems, a wave buoy (mark ◎) has also been deployed at depth of 12.5m[17]. The wave buoy was deployed to compare the directional spectrum estimated from Doppler spectra by BM and MBM across the region.

Hashimoto et al [5] reported that the observation was carried out for 5 minutes at each station and repeated every twenty minutes providing 896 coherent samples at each measurement point. To

estimate the Doppler spectra, 512 sample FFTs were used with a 75% overlap to provide 4 spectra for each five-minute period. Three successive five minute collections were then averaged to provide an hourly averaged (from 12 individual) Doppler spectrum. In SCAWVEX, the method developed by Longuet-Higgins et al[19] was used to analyze the directional wave data measured by buoy. The resultant Fourier coefficients for the directional spectra have been preserved as the parameters of the directional spectra. Based on these Fourier coefficients, we applied the method developed by Kim et al[20] to obtain the directional spectra using the Maximum Entropy Principle method[12]. Details of the analysis of the wave data and computations of the directional wave spectra with BM can be found in the previous study reported by Hashimoto et al[5].

5.2 Directional Spectrum Estimations

Throughout this work, the nonlinear inversion with the BM and MBM developed by Hashimoto and Tokuda[3] and Lukijanto et al[11] respectively are applied to the Doppler spectra measured in the SCAWVEX data as mentioned above. In the following, we estimate the directional spectra from observed points A to I as shown in **Fig. 4** in order to verify the applicability and accuracy of the both methods.

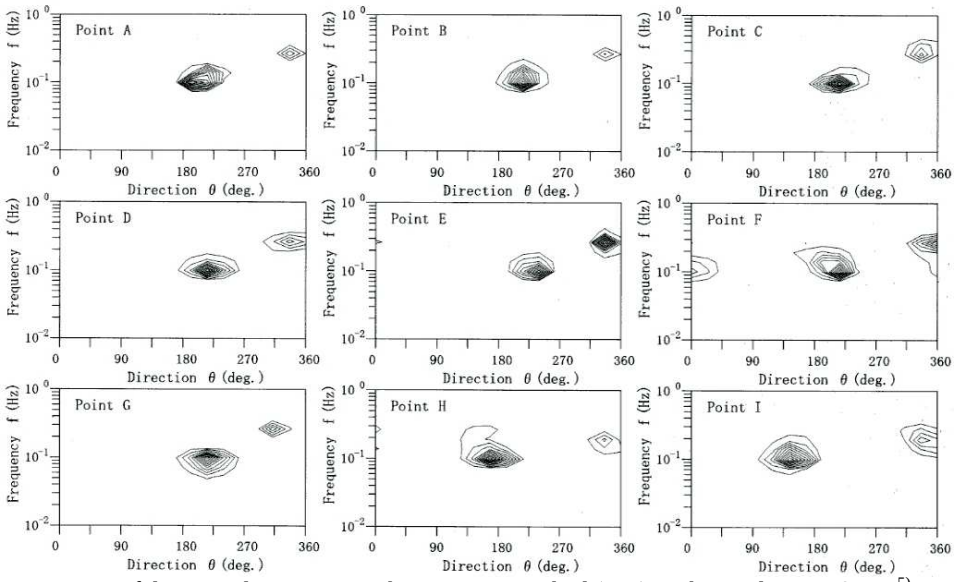

Fig. 5. Estimation of directional wave spectra by Bayesian Method (BM) at observed points A to I[5].

Doppler spectra used in this study were analyzed using procedures as described in Hashimoto et al[5], in which the reliable directional spectra at observed points A to I were successfully estimated by BM widely distributed in those areas, as shown in **Fig. 5**. The results showed that directional spectra could be measured consistent in the proper directions with the swell and the wind waves propagating.

It should be noted that for each numerical computation by using BM, the accuracy of numerical estimation depends on the assumed number of parameters. However, for instance, in the case of M=N=16, the computation time required was about ten seconds which is permissible for practical use. Meanwhile, in the case of M=N=32, the computation time took several minutes which is presently impractical for real time processing. Consequently, the original BM is required to be

modified in order to overcome the disadvantage. For that reason, the MBM has essentially been developed.

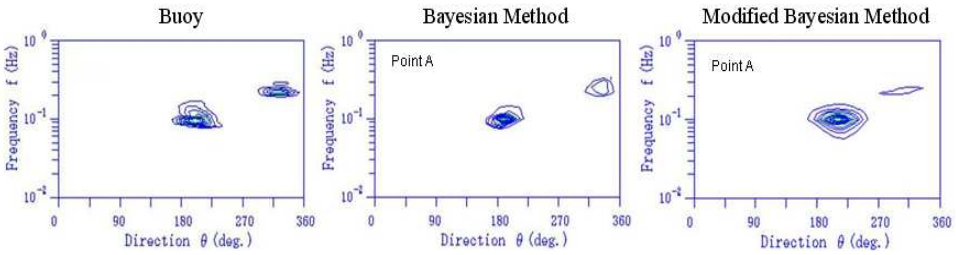

Fig. 6. Comparison of the directional spectra between buoy with BM and MBM at observed point A. (The contour lines are drawn for every 1/10 of the range from 0 to maximum value of the directional spectrum)

Before the MBM was applied to all observed point A to I, Lukijanto et. al[21] first estimated the directional spectra at observed point A by using BM and MBM for comparing the directional spectrum measured with wave buoy. The results showed that the directional spectrum measured with buoy and the directional spectrum estimated by BM and MBM showed good agreement. Almost similar shape was observed by three different methods (buoy, BM and MBM), even though the estimated frequency spectra were found a little bit different. The directional energy distribution estimated by BM and MBM were almost consistent with the one measured with buoy, where the main peaks were found also in a good agreement as shown in **Fig. 6**.

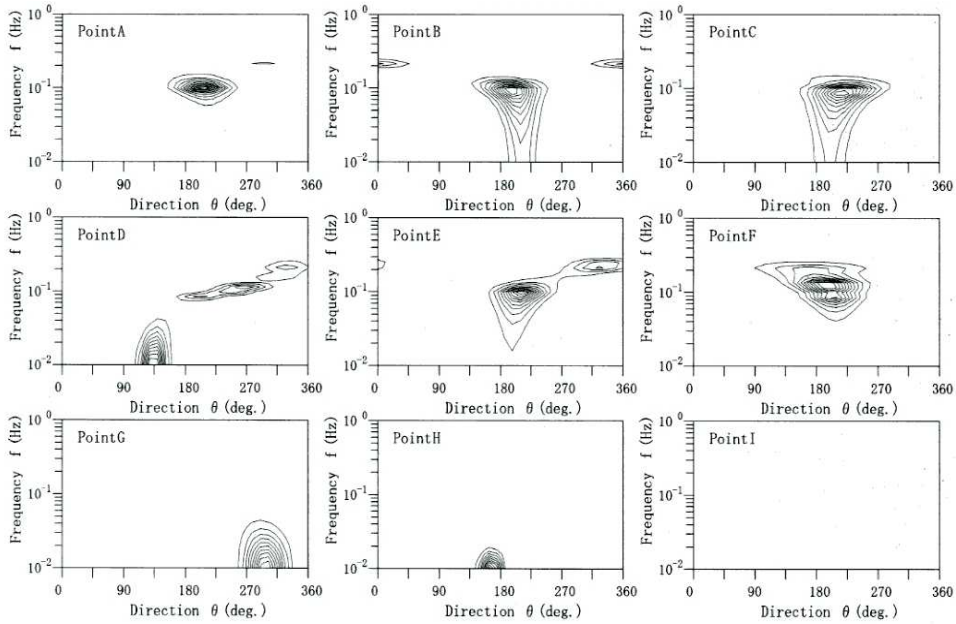

Fig. 7. Examples of the directional spectra estimated by Modified Bayesian Method (MBM), before the boundary value at the lower frequency are given.

Furthermore, the MBM was examined by applying all observed points A to I. The results show that the directional spectrum at observed point A is quite good, as drawn in **Fig. 7**. It might be that the location of observed point A was not so far from the radar locations and the signal to noise ratio seemed to be high so that the reasonable directional spectrum could be well estimated. Unfortunately, the results were not always suitable when the MBM were applied to other observed points. In other words, strange directional spectra are obtained at observed points B to I.

The possible explanation for such features occurred may be that Doppler spectra may include little information of the lower frequency component. That is, the Doppler radar measures wave component having the wave-length of about 6 m. For that reason very long waves may not possible to measure. In actuality, there was little energy in frequency spectrum measured with buoy[5]. On the other hand, as described in Eq. (28) in section 3.2, the directional spectrum is assumed as an exponential function having the power expressed by a Fourier series over the direction and the piecewise constant function over the frequency. In such case, the exponential function may not estimate suitable directional spectrum. Thus, by using the expression of the exponential function may be difficult to express the value close to zero at the lower frequency side[21]. Consequently, the numerical instabilities might occur in these particular cases.

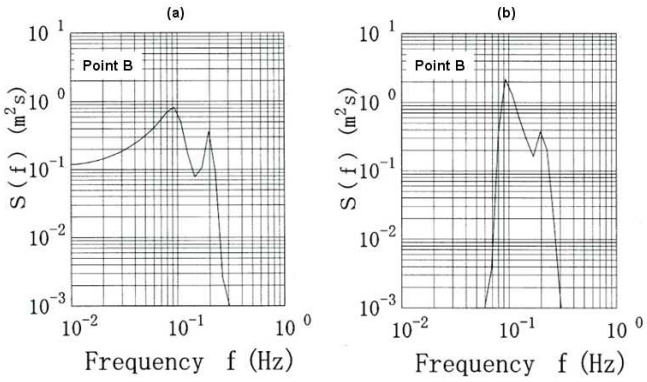

Fig. 8. The frequency spectrum at observed point B; (a) the actual condition before the boundary value is given at the lower frequency and (b) the improved result after applying the boundary value.

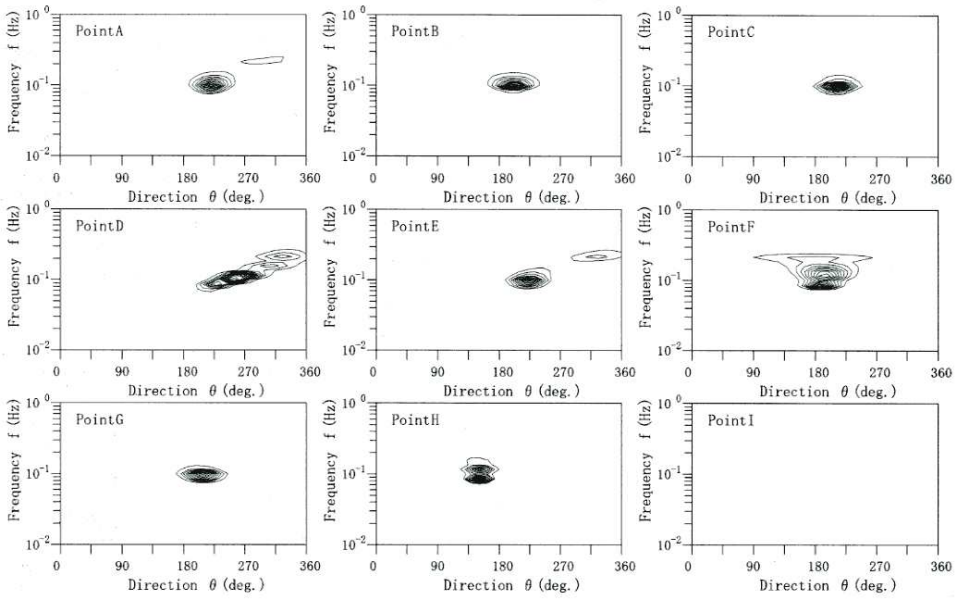

Fig. 9. Examples of the directional spectra estimated by Modified Bayesian Method (MBM), after the boundary value at the lower frequency are applied.

Figure 8.a shows an example of the instability occurred at observed point B which corresponds to the **Fig. 7**. The numerical instability is shown clearly at the lower boundary frequency, as shown in **Fig. 8.a**. Since there is very little energy at this lower boundary, therefore to

eliminate the instability at lower frequency, a definite value may be given as the boundary condition. **Figure 8.b** is an example of the estimated spectrum where the boundary condition was given as $S(f,\theta)=10^{-3}\left(\mathrm{m^2s}\right)$ at $f=10^{-2}$ (Hz). A proper frequency spectrum can be estimated. Furthermore, the similar technique was applied to all observed points A to I in order to examine the usefulness of the method as described above.

As shown in **Fig. 9,** generally the directional spectra and the peaks of frequency spectrum are properly estimated by MBM at the proper frequencies with that observed by buoy. The observed points A to G appeared also at the proper directions with winds. Exceptional case was only at observed point I where the iterative computation failed. Incidentally, on the other hand according to the Hashimoto et al (2003)[5] among all the observation points, the iterative computations by BM for observed point A to I converged, as shown in **Fig. 5**.

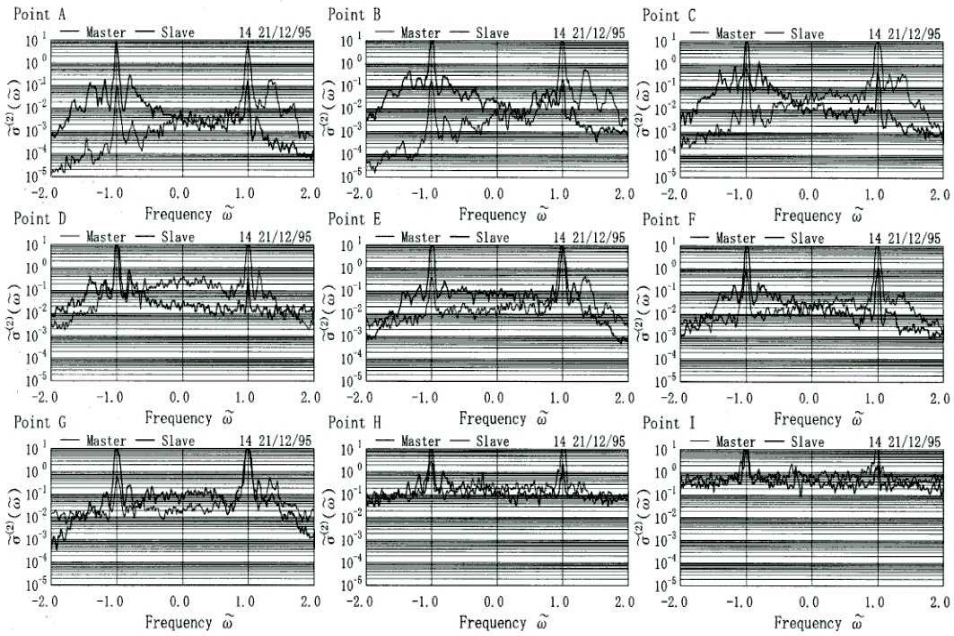

Fig. 10. Examples of the normalized Doppler spectra of the backscatter at observed points A to I from two radars at Master and Slave point.

Figure 10 shows the Doppler spectra correspond to the **Fig. 9**. As seen in **Fig. 10**, the first order Doppler spectral component are clearly seen around the second order component at observed points A to G. Note that at observed points H and I, the quality of the signal to noise might be very low and contaminated with noise because their locations were very far from the radar. Therefore, a reliable second order Doppler energy spectrum might not be measured during the observation. However, Hashimoto et al[5] succeeded to estimate the directional spectra by using BM, on the basis of the same Doppler spectra at all observed points A to I with high accuracy. The results of our study suggest that the BM is more robust in presence of noise (e.g. at points H and I) than MBM.

In addition, it should be noted that the comparison of computation time of those directional spectra in **Figs. 5** and **9,** the MBM is found to be an efficient method for estimating directional spectra because it computes much faster than BM. However, the accuracy of directional spectrum estimated by BM seems a bit better than MBM.

6. Conclusions

One of the intentions of this paper is to compare the performance of two inversion methods qualitatively, i.e. BM and MBM, developed by Hashimoto and Tokuda (1999) and Lukijanto et al (2009a) respectively by identical twin experiments. The results clearly demonstrate that the directional wave spectra can be estimated by both methods on the basis of the Doppler spectra. In terms of computational costs and memory requirements, both methods have been found to differ greatly. The comparison suggested that the MBM was more efficient than the BM since the MBM is capable of executing high speed computing and reducing the memory usage. Therefore, the MBM has a good potential for operational application. Although, the BM is considered to be impractical because of its time consuming iterative computations, but the BM is accurate method to estimate directional spectra.

The BM and MBM were successfully verified with the reliable data obtained from SCAWVEX project. Comparisons between the BM and MBM have shown good agreement with the estimated directional spectrum measured with buoy. Indeed, both methods show reasonably good for estimating directional wave spectra from HF ocean radar. However, especially for the MBM, the numerical instability might occur at the lower boundary where the signal to the noise ratios is quite bad. Although we solved this problem by giving a boundary condition at the lowest frequency of directional spectrum, more efforts are still underway to overcome the instability.

It is interesting to note that, although the BM shows very time consuming in doing the computations, the BM is more robust against the presence of noise than the MBM. Further works involving these studies, verification of the MBM is being undertaken for validating to the actual field data with a number of different radar systems in a number of different locations.

Acknowledgements

The authors sincerely wish to express their appreciation to Prof. L.R.Wyatt, from School of Mathematics and Statistics, The University of Sheffield, UK, as the principal scientist of the organizations involved in the Surface Current and Wave Variability Experiments (SCAWVEX) project for her kind support to provide reliable field data.

References

1) Crombie; Doppler spectrum of sea echo at 13.56Mc/s, Nature, vol. 175, pp. 681-682. (1955)
2) Barrick, D. E.; Remote sensing of sea state by radar, Remote sensing of the Troposphere, V. E. Derr, Editor, U. S. Govt. Printing Office, Washington, D. C., 12. (1972).
3) Hashimoto, N. and Tokuda.; A Bayesian approach for estimation of directional wave spectra with HF radar., Coastal Engineering Journal, vol. 41, no. 2, pp. 137-147. (1999).
4) Hashimoto, N, Lukijanto, Yamashiro, M. and Kojima, S.; Development of A Practical Method for Estimating Directional Spectrum from HF Radar Backscatter. Journal of Coastal Engineering 55 (1). pp. 1451-1455. (2008).
5) Hashimoto, N., Wyatt, L. R and Kojima, S.; Verification of Bayesian method for estimating directional spectra from HF radar surface, Coastal Engineering Journal (45), no.2, pp. 255-274. (2003).

6) Hisaki, Y.; Nonlinear inversion of the integral equation to estimate ocean wave spectra from HF radar, Radio Science, Vol. 31, No.1, pp. 25-39. (1996).
7) Howell, R and Walsh, J.; Measurements of Ocean Wave Spectra Using Narrow-Beam HF Radar, IEEE Oceanic Engineering Journal. Vol.18, No.3, pp. 296-305. (1993).
8) Lipa, B. J. and Barrick, D.E.; Extraction of sea state from HF radar sea echo: Mathematical theory and modeling, Radio Science, vol. 21, no. 1, pp. 81-100. (1986).
9) Wyatt, L.R.; A relaxation method for integral inversion applied to HF radar measurement of the ocean wave directional spectrum, International Journal of Remote Sensing. (11), no. 8, pp. 1481-1494. (1990).
10) Hashimoto, N.; Analysis of the directional wave spectrum from field data, Advances in Coastal and Ocean Engineering, vol. 3, World Scientific, pp. 103-143. (1997).
11) Lukijanto, Hashimoto, N. and Yamashiro, M.; Further Modification Practical Method of Bayesian method for estimating directional wave spectrum by HF radar. Proc. 19th ISOPE (Intl. Offshore (Ocean) and Polar Eng.) pp. 898-905 (2009a).
12) Hashimoto, N. and Kobune.; Estimation of Directional Spectra from the Maximum Entropy Principle, Proc. 5th Int. Offshore Mech. and Arctic Eng. Symp. Vol. 1, pp. 80-85., (1986).
13) Lipa, B. J. and Barrick, D.E.; Analysis Methods for Narrow-Beam High-Frequency Radar Sea Echo, NOAA Technical Report ERL 420-WPL 56, pp. 1-55. (1982).
14) Hashimoto, N., Kobune and Kameyama.; Estimation of directional spectrum using the Bayesian approach and its application to field data analysis, Report of PHRI, 26, 5, pp. 57-100. (1987).
15) Barrick, D. E.; Extraction of wave parameters from measured HF radar sea-echo Doppler spectra, Radio Science, Vol. 12, No.3, pp. 415-424. (1977).
16) Akaike, H.; Likelihood and Bayesian procedure, Bayesian Statistics (Bernardo, J. M., De Groot, M., Lindley, D.U. and Smith, A.F.M) University Press, Valencia, pp. 143-166 (1980).
17) Wyatt, L. R. Gurgel, K.W., Peters, H.C., Prandle, D., Krogstad, Haug, O., Gerritsen, Wensink.; The SCAWVEX Project. Proc.of WAVES97, ASCE (1997).
18) Wyatt, L.R.; The Ocean Wave Directional Spectrum, Oceanography Journal, vol. 10, no. 2, pp. 85-89. (1997).
19) Longuet-Higgins, M. S., D. E. Cartwright and N. D. Smith.; Observations of the directional spectrum of sea waves using the motion of a floating buoy, Ocean Wave Spectra, Prentice-Hall, Inc., pp.111-136 (1961).
20) Kim, T., L.-H. Lin and H. Wang.; Application of Maximum Entropy Method to the Real Sea Data, Coastal Engineering 1994, Vol. 1, ASCE, pp. 340-355 (1994).
21) Lukijanto, Hashimoto, N. and Yamashiro, M.; An Improvement of Modified Bayesian Method for estimating directional wave spectra from HF Radar Backscatter. Proc. 5th APAC (Asian and Pacific Coasts), pp. 105-111 (2009b).